Hybrid Switched-capacitor Three-phase Direct AC-AC Converter with Adjustable Output Voltage

Guanyu Yan
Northeast Electric Power University
Ruifeng Li
17643208037@163.com
Northeast Electric Power University
Chuang Liu
Northeast Electric Power University
Dongbo Guo
Tsinghua University
Mulin Han
Northeast Electric Power University
Fengyue Zhao
Northeast Electric Power University

Article

Keywords: Direct ac/ac converter, three phase, switched capacitor (SC).

Posted Date: October 7th, 2025

DOI: https://doi.org/10.21203/rs.3.rs-7760201/v1

Additional Declarations: No competing interests reported.

Hybrid Switched-capacitor Three-phase Direct AC-AC Converter with Adjustable Output Voltage

Guanyu Yan[1,2], Ruifeng Li[1,*], Chuang Liu[1], Dongbo Guo[3], Mulin Han[1], Fengyue Zhao[1]

[1]College of Electrical Engineering, Northeast Electric Power University, Jilin, 132012, Jilin, China
[2]College of Electrical and Information Engineering, Beihua University, Jilin, 132013, Jilin, China
[3]Department of Electrical Engineering, Tsinghua University, Haidian District, 100084, Beijing, China
*e-mail：17643208037@163.com

Abstract

A switched-capacitor (SC) three-phase direct ac/ac converter is presented in this paper. It includes an additional inductor and two SC cells for each phase. Due to the introduction of the inductor, the output voltage can be adjusted. The proposed converter operates in fixed switching frequency. One of the features of this topology is that the voltage stresses across the switches and capacitors equal half of high-side voltage. In addition, self-balancing capability of capacitor voltages and simple modulation strategy are other characteristics. The main advantage of the proposed converter is the employment of unidirectional switches (a single MOSFET), which avoids the commutation problems in the bidirectional switches. A detailed description of the operation principle, quantitative analysis, and design considerations for the proposed converter is provided. Eventually, a prototype with 55V/220V and 3kW is designed to demonstrate the feasibility and validity of the proposed converter.

Key Words

Direct ac/ac converter, three phase, switched capacitor (SC).

Introduction

As the penetration of distributed renewable energy like photovoltaic and wind power expands, power quality concerns including voltage swell/sag and voltage fluctuations are attracting increasing attention [1]. Moreover, the growth, diversity, and sensitivity of loads also impose higher requirements on power quality [2]. Transformers, as commonly used devices in distribution networks, can achieve voltage adjustment between power grid and equipment. If electrical isolation is not necessary, autotransformers are often employed to supply three-phase voltage to the loads. These devices have the disadvantages such as high cost, large size, saturation, and high inrush current [3]. Furthermore, poor controllability and slow dynamic response fail to meet the voltage stability requirements of sensitive loads [4]. Therefore, as a key equipment of renewable energy generation and utilization, the power electronic converter plays a vital role in resolving the above problems. The ac/ac converters, as an important branch of power electronic converters, are widely applied in industrial and commercial fields. The initial ac/ac conversion was performed by the employment of thyristor power converters, which can regulate the output voltage by implementing the phase angle control on the input voltage [5]. Nevertheless, these converters present some notable drawbacks, such as low voltage gain, poor harmonic performance and low efficiency [6,7]. In order to avoid these disadvantages of the thyristor power converters, a large number of the PWM ac/ac converters have been proposed. These PWM ac/ac converters, as alternatives to transformers/autotransformers, can be generally divided into three categories: the indirect ac/ac converters [8-11], matrix converters [12-15] and the direct ac/ac converters [16-19]. The indirect ac/ac converter is a two-stage power converter, which requires a dc link to decouple the input and output. Therefore, this converter can adjust both the amplitude and frequency of the voltage. However, the dc link increases the volume and maintenance requirements of the converter. Consequently, in applications where only voltage amplitude adjustment is required, the benefits of the indirect converters are not significant. Matrix converters can regulate both the voltage amplitude and frequency simultaneously, but they usually exhibit obvious drawbacks such as complex modulation strategies, low voltage gain and input current THD [20-22]. Due to the absence of a dc link, the direct ac/ac converter is a single-stage conversion that has the advantages such as compact size, low cost, high efficiency, and high power density. This makes it more attractive for applications that only require adjusting voltage amplitude. The buck, buck-boost, and Cuk converters proposed in [18,19,23] have the characteristics of simple circuits and high efficiency. Nevertheless, due to the adoption of bidirectional switches, the components in the circuit may suffer from overvoltage stress, which can significantly degrade the reliability of these converters. Although the Z-source converters could achieve high voltage gain, they still have the commutation issues owing to the employment of bidirectional switches [24-26].

The switched-capacitor converters (SCCs) were originally proposed for dc/dc conversion in low-voltage and low-power applications [27,28]. Subsequently, a variety of topologies have been applied in dc/dc, dc/ac and ac/dc. As most SCCs do not incorporate inductive components and only employ switches and capacitors, they present advantages such as simple structure, compact size, and high efficiency. Therefore, the SCCs have attracted widespread attention, and some applications have already benefited from them. The equivalent circuit models were developed in references [29-31] to facilitate the description and analysis of SCCs behaviors. Furthermore, several publications have discussed the impact of circuit parameters on SCCs, which can help to improve the performance of SCCs [32-34]. Recently, the SC principle was introduced into the direct ac/ac converters. Reference [35] presents a single-phase direct ac/ac converter, which consists of two SC legs and can achieve a voltage conversion ratio of 1/2 or 2. It is characterized by the employment of unidirectional switches, differential connection and low voltage stress across the components. Reference [36] proposes another non-differential bidirectional SC ac/ac converter composed of one SC and four bidirectional switches, which achieves the same voltage conversion ratio as reference [35]. The SCCs in the aforementioned references exhibit a fixed voltage conversion ratio. By introducing magnetic components, reference [37] develops a hybrid boost SCC that can adjust the output voltage by varying the duty cycle. A SC three-phase ac/ac converter was proposed in reference [38], which is derived from reference [36]. It consists of three modules, each containing 3 capacitors and 4 bidirectional switches. The modules can be connected in either wye or delta configuration. Reference [39] presents another SC three-phase ac/ac converter with open-delta configuration. Compared to reference [38], it achieves a one-third reduction in component count. According to reference [35], a reduced switch count SC three-phase ac/ac converter was reported in reference [40]. Due to the adoption of the differential structure, the introduced dc component enables the employment of unidirectional switches, which reduces the number of switches compared to references [38,39]. In summary, the results from references [35-40] are promising, and demonstrate that the SC ac/ac converter can provide a new and effective solution for replacing traditional autotransformer, particularly in scenarios where only voltage amplitude regulation is required. However, the SC three-phase ac/ac converters with adjustable output voltage have not yet been reported.

This paper presents a SC three-phase direct ac/ac converter. An important characteristic of the proposed converter is the differential connection, which introduces dc components across all capacitors and switches. Due to no negative voltages across the capacitors and switches, unidirectional switches can be employed in the converter. Without bidirectional switches, the converter requires only a simple modulation strategy to avoid commutation issues. Furthermore, the switches and capacitors in this converter only withstand low voltage stresses. The capacitors can achieve self-balanced voltages. On account of the inclusion of a small magnetic component, the converter can realize a controllable output voltage by varying the duty cycle.

The rest of this paper is arranged as follows: in section 1, the topology of the proposed converter and PWM modulation strategy are presented. In addition, the operation of the proposed converter is analyzed. In section 2, the quantitative analysis is discussed. Then the design considerations of the key components are analyzed in section 3. Subsequently, the experimental results are reported in section 4. Finally, the conclusion is given in section 5.

1. Description Of the Proposed Three-Phase direct AC/AC Converter

1.1 Topology description and PWM modulation strategy

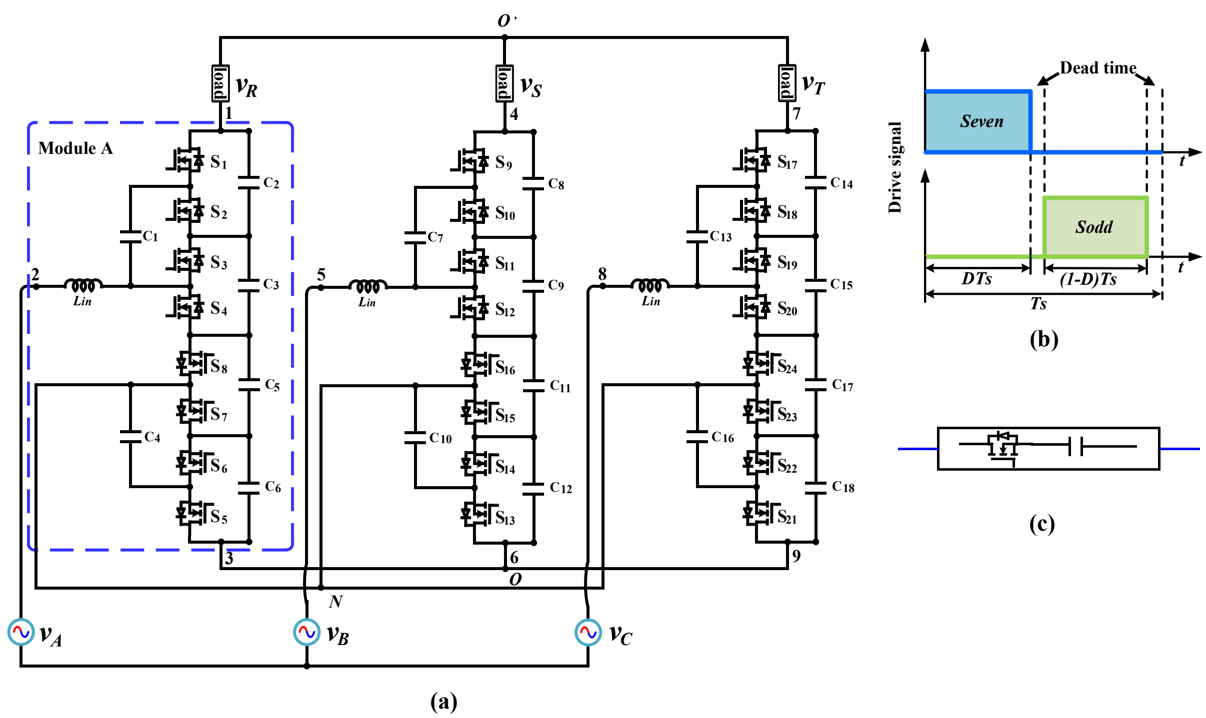

Figure 1. (a) Proposed SC three-phase ac/ac converter; (b) PWM drive signals; (c) Simplified symbol for a module.

The proposed topology consists of three modules with a wye connection. The input voltages (v_A, v_B and v_C) are connected at points 2, 5, and 8, and the load voltages (v_R, v_S and v_T) are available at points 1, 4, and 7. Each phase is represented by one module. For instance, phase A is denoted by module A as illustrated in Figure 1(a). Each module is composed of an input inductor (L_{in}) and two symmetrical switched capacitor cells (2 switched capacitors, 4 output capacitors and 8 switches). Therefore, the entire converter has 3 input inductors, 18 capacitors (C_1~C_{18}) and 24 switches (S_1~S_{24}). Owing to the lack of available path for the current, direct ac/ac converters usually suffer from the commutation problems, which will lead to voltage spikes across the components [41]. Hence, complex modulation strategy or snubber circuits are required to overcome this problem. Due to the absence of bidirectional switches in the proposed converter, this converter only needs a simple PWM modulation strategy to avoid the commutation problems. Consequently, the employed modulation strategy is shown in Figure 1(b), in which switches S_{even} and S_{odd} are driven in a complementary manner during one switching period. Besides, a dead time is needed to prevent the shoot-through issue. Regardless of the direction of the current, there is always a current path in the converter, which can improve the reliability of this converter. Figure 1(c) shows the simplified symbol to denote a module and will be used in Figure 4.

1.2 Operation principle

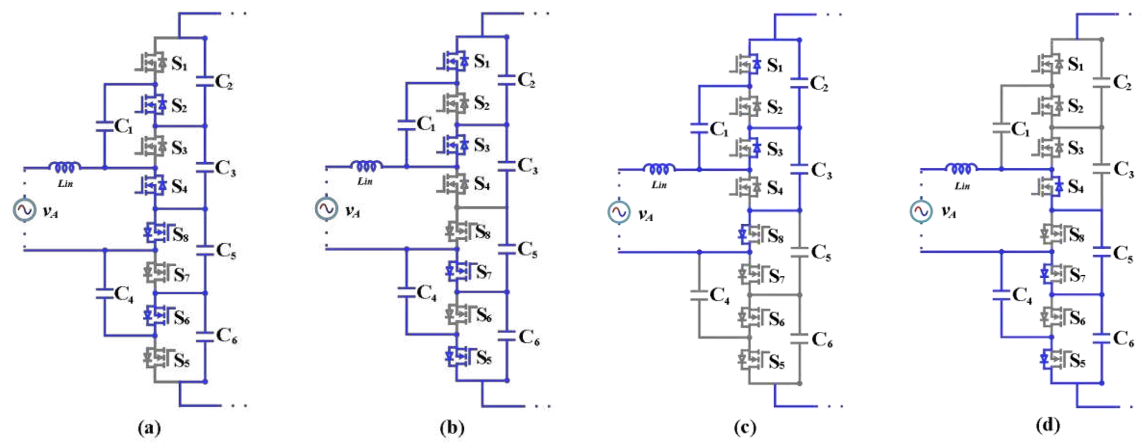

Figure 2. Operational stages for module A. (a) Stage I: even switches are in on-state; (b) Stage II: odd switches are in on-state. Circulating path for the inductor current i_L during dead time. (c) $i_L>0$; (d) $i_L<0$.

The proposed converter has the same three operational stages for each module in a switching period. Therefore, the analysis made here is only for module A during the positive half-cycle of the input voltage, which is shown in Figure 2. For the negative half-cycle, the module A presents the same operational stages except for the opposite current direction. The operational stages are described as follows.

Stage I ($0<t<DT_s$) starts when S_2, S_4, S_6 and S_8 are in on-state while S_1, S_3, S_5 and S_7 are in off-state. The input inductor L_{in} is directly connected to input voltage v_A and stores the energy. The capacitor C_1 is in paralleled connection with C_3. Similarly, the capacitor C_4 is connected in parallel with C_5. Capacitors C_2 and C_6 provide energy to the load during the whole DT_s interval. Switches S_2, S_4, S_6 and S_8 are turned-off by the end of stage I.

Stage II ($DT_s<t<T_s$) starts when S_1, S_3, S_5 and S_7 are in on-state while S_2, S_4, S_6 and S_8 are in off-state. The input inductor L releases the energy. The capacitor C_1 transfer the energy to C_2 and the load. The capacitor C_4 is charged by C_6. As capacitor C_3 has been discharging the energy in the stage I, it will be charged during this stage. Likewise, capacitor C_5 will discharge the energy in this stage. Switches S_1, S_3, S_5 and S_7 are turned-off at the end of stage II.

In order to prevent the shoot-through problem, it is crucial to add an appropriate dead time denoted as stage III between the above two stages. If the input inductor current is positive, the body diodes of S_1 S_3, and S_8 can provide the circulating path for the inductor current as shown in Figure 2(c). In the same way, the body diodes of S_4 S_5, and S_7 can conduct the negative inductor current as well, which is illustrated in Figure 2(d). One switching period consists of the above stages.

1.3 Operation characteristic

By observing Figure 1(a), it can be seen that the middle part of each module is a boost converter, connected with two SC cells. Thus, the theoretical voltage gain of the module A is represented by (1). The other two modules have the same voltage gain.

$$G_A = \frac{v_{13}}{v_A} = \frac{2}{1-D} \tag{1}$$

Considering the duty cycle D=0.5, the input and output voltages of each module are shown in Figure 3, where V_{max} is the maximum value of the output voltage v_{13}. For module A, the voltage v_{13} is applied to capacitors C_2, C_3, C_5 and C_6. Therefore, equations (2) and (3) can be achieved.

$$v_{c2} + v_{c3} - v_{c5} - v_{c6} = v_{13} \tag{2}$$

$$v_{c2} + v_{c3} + v_{c5} + v_{c6} = V_{\max} \tag{3}$$

As mentioned previously, the capacitor C_1 will be connected to capacitors C_2 and C_3 respectively within a switching period and similarly, the capacitor C_4 will be connected to capacitors C_5 and C_6 respectively during the same switching period. In other words, the switched capacitor C_1 can maintain the voltage balance across C_2 and C_3, while C_4 can keep the voltage balance across C_5 and C_6. This operation principle of module A can also apply to the modules B and C. Therefore, rearranging equations (2) and (3), and collecting terms, equations (4) and (5) can be yielded for module A.

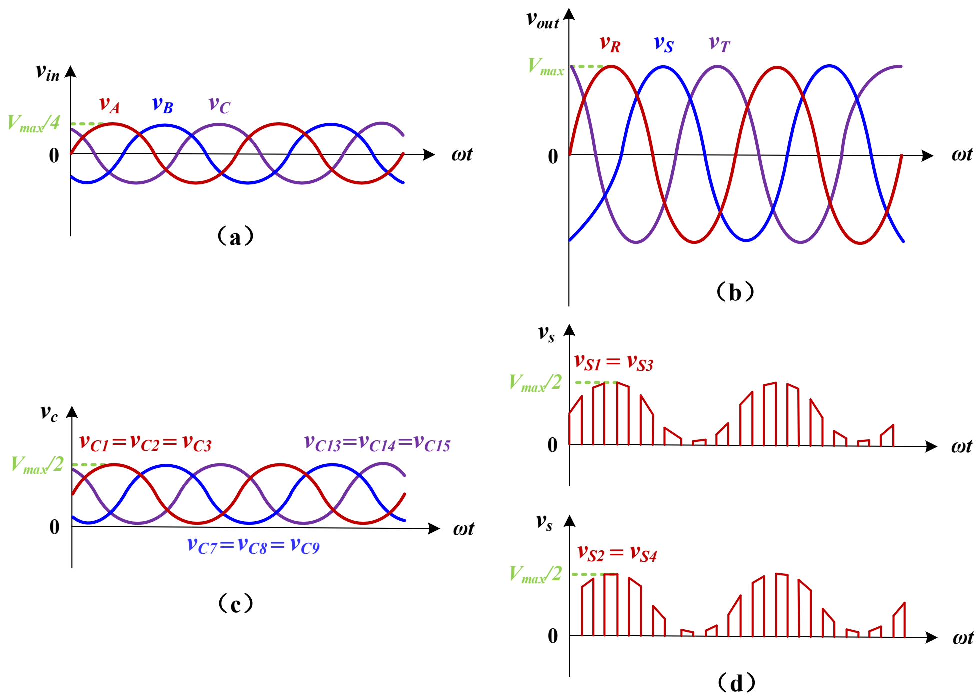

Figure 3. Theoretical voltage waveforms of the proposed converter. (a) Input voltages; (b) Output voltages; (c) Voltages across capacitors; (d) Voltages across switches.

$$v_{c1} = v_{c2} = v_{c3} = \frac{1}{4}V_{\max} + \frac{1}{4}v_{13} \tag{4}$$

$$v_{c4} = v_{c5} = v_{c6} = \frac{1}{4}V_{\max} - \frac{1}{4}v_{13} \tag{5}$$

As can be seen from equation (4), due to the differential connection, a dc component of $1/4V_{max}$ is introduced into the capacitors. Moreover, capacitors C_1, C_2, and C_3 are in phase with the input voltage v_A and have an ac component of $1/4v_{13}$. Therefore, the total capacitor voltages C_1, C_2, and C_3 are equal, each consisting of an ac component and a dc component. Their maximum values are equal to $1/2V_{\max}$, which is another advantage of the proposed converter. In the same way, capacitor voltages C_4, C_5, and C_6 have the same features, but they are out of phase with input voltage v_A as described in equation (5). The capacitor voltages of modules B and C are the same as those of module A, except they are phase-shifted by -120° and +120° with respect to v_A respectively as shown in Figure 3(c). All switches present the same shape as their corresponding capacitor voltages with the maximum value $1/2V_{\max}$, but they are high frequency quantities. The voltage waveforms of the switches S_1, S_2, S_3 and S_4 in module A are illustrated in Figure 3(d).

1.4 Module Configuration

In order to maintain the differential characteristic between the input and output, the three modules can only present a wye configuration. However, the three-phase load can be connected through a delta or wye connection. Therefore, there are two possible configurations (wye-delta and wye-wye) for the proposed converter. Different module-load connections lead to different voltage phasor configurations. Considering D=0.5, the voltage gain and phase shift between the input and output voltages are analyzed for each configuration. The detailed results are listed in Figure 4.

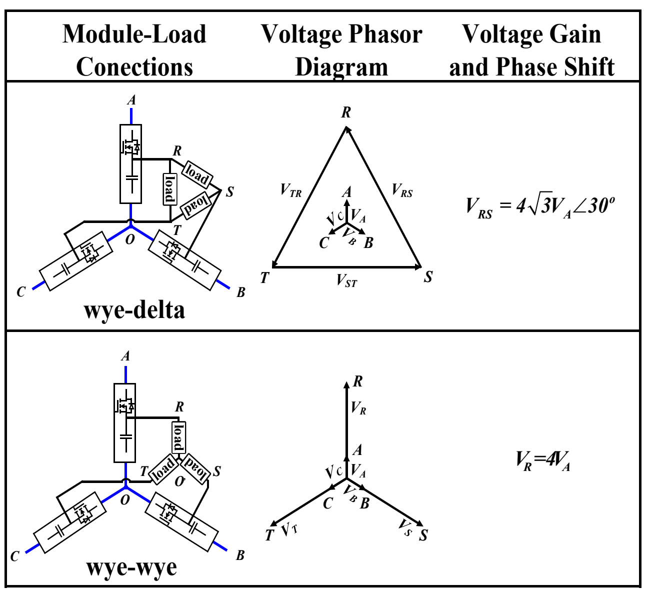

Figure 4. Analysis of voltage phasor for different module-load connections(D=0.5)

2. Quantitative Analysis

2.1 Operational modes of the proposed three-phase converter

According to the charging or discharging capacitor current, the SC cell can be categorized into three operational modes: no charge (NC), partial charge (PC) and complete charge (CC) [30,31]. The CC mode indicates that the capacitor will complete the entire charging or discharging process, which leads to a high current and thereby reduces the efficiency. Hence, the CC mode is not recommended. In contrast, there is a low constant capacitor current value in NC mode, which can help improve the efficiency. Nevertheless, a large capacitor or high switching frequency is required in this mode, which will increase the costs. Capacitors are only partially charged in the PC mode. Compared to the NC mode, PC mode demonstrates similar advantages while requiring relatively lower capacitance and switching frequency. Therefore, the PC mode is a good choice for SC cell [36]. The charging/discharging capacitor current will approach zero within a time interval of 5τ [36,42]. τ is the time constant of the SC cell, which is represented by equation (8). To make the proposed converter operate in PC mode, the charging or discharging time interval must be less than 5τ, yielding.

$$DT_s \le 5\tau \tag{6}$$

$$(1-D)T_s \le 5\tau \tag{7}$$

$$\tau = (2R_{DS(on)} + R_{ESR})C \tag{8}$$

where $R_{DS(on)}$ is the conduction resistance of one MOSFET switch, R_{ESR} is the equivalent series resistance of a capacitor, C is the capacitance for each capacitor utilized in the converter (all equal capacitors).

2.2 Equivalent circuit

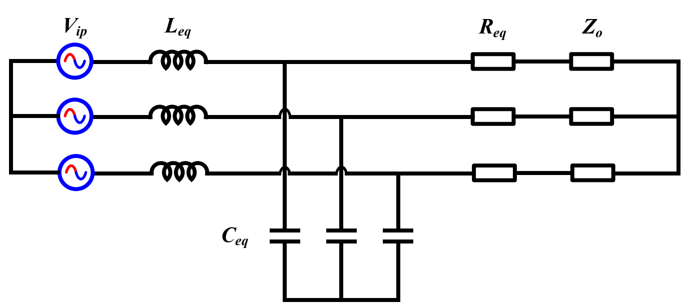

Figure 5. Three-phase equivalent circuit for wye-wye connection.

Under the condition of a balanced three-phase load, a three-phase equivalent circuit model seen by the load side with a wye-wye connection between the module and the load is established in Figure 5. This model includes the input equivalent inductors L_{eq}, the equivalent capacitances C_{eq}, the equivalent resistances R_{eq} and the output loads Z_o. For analytical convenience, the duty cycle D is set to 0.5. The input line-to-neutral voltage is denoted by three voltage sources v_{ip} in wye configuration, which is four times the input line-to-neutral voltage from the grid side. The resistances R_{eq} represent the conduction losses caused by SCs in each module during the charging and discharging processes [33]. Within each switching period, the voltage across the capacitor can be regarded as approximately constant.

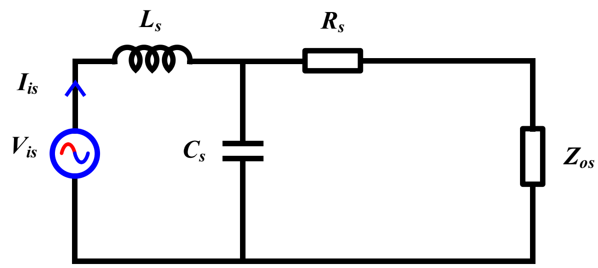

Figure 6. Proposed single-phase equivalent circuit.

Since the proposed converter shares the same operational process as the dc/dc SCC, its equivalent resistance R_{eq} is similar to that reported in previous studies [32,33]. As mentioned earlier, for module A, capacitor C_1 is connected in parallel with C_3 and C_2 during DT_s and $(1\text{-}D)T_s$ respectively. Therefore, capacitor C_1 can be equivalent to the value of DC_1 and $(1\text{-}D)C_1$ in parallel with capacitors C_3 and C_2, respectively [36]. Likewise, capacitor C_4 also has a value of DC_4 and $(1\text{-}D)C_4$ to be connected to C_5 and C_6 separately. Considering D=0.5 and all equal capacitors, the equivalent capacitance C_{eq} for each module can be obtained in this manner. The parameters of the three-phase equivalent circuit seen by the load side are listed as follows

$$R_{eq} = \frac{1}{2 f_s C} \frac{(e^{\frac{1}{f_s \tau}} - 1)}{(1 - e^{\frac{D}{f_s \tau}} - e^{\frac{1-D}{f_s \tau}} + e^{\frac{1}{f_s \tau}})} \tag{9}$$

$$L_{eq} = 16 L_{in} \tag{10}$$

$$C_{eq} = \frac{3C}{8} \tag{11}$$

where f_s is the switching frequency. To facilitate the analysis of different load connections, the proposed three-phase equivalent circuit can be simplified into a single-phase one as shown in Figure 6, where this single-phase circuit handles only one-third of the total output power. Its parameters can be calculated by using the equations mentioned above. The input voltage source is represented by v_{is}, the conduction losses are denoted by R_s, the reactive power in the circuit is represented by L_s and C_s, and the output resistance is denoted by Z_{os}. Their specific values are listed in Table 1.

Connections (module-load)	v_{is}	L_s	C_s	R_s	Z_{os}
wye-wye	v_{ip}	L_{eq}	C_{eq}	R_{eq}	Z_o
wye-delta	v_{ip}	L_{eq}	C_{eq}	R_{eq}	$Z_o/3$

Table 1. Parameters for single-phase equivalent circuit

The analysis of the equivalent circuit illustrated in Figure 6 allows the derivation of key parameters, which are crucial for designing the proposed converter and will be discussed in the next section. These parameters also provide essential insights into the performance and characteristics of the proposed converter.

2.3 Comparisons with other SC three-phase ac/ac converters

Topology	Proposed converter	Ref. 38	Ref. 39	Ref. 40
Inductor count	1	0	0	0
Adoption of bidirectional switches	No	Yes	Yes	No
Switch count	24	24	16	12
Frequency	Fixed	Fixed	Fixed	Fixed
Capacitor count	18	9	6	9
Voltage stresses	$V_p/2$	$V_p/2$	$V_p/2$	V_p
Voltage regulation	Yes	No	No	No
Voltage gain	2/(1-D)	2 or 0.5	2 or 0.5	2 or 0.5
Complexity of modulation	Low	Low	Low	Low

Table 2. Comparisons between the proposed converter and other converters

Table 2 lists some features comparisons between the proposed converter and other converters. Due to the adoption of an additional inductor, the proposed converter can regulate the output voltage compared to other topologies. The voltage gain of each module in the proposed converter is twice that of those reported in [38,39] at the expense of more capacitors and switches (D=0.5). The maximum voltage of corresponding topology in the high voltage side is represented by V_p. It can be observed from Table 2 that this paper shares the same advantage of low voltage stresses across the components with [38,39]. Moreover, another advantage of the proposed converter is the employment of unidirectional switches, which avoids the commutation problems of bidirectional switches and improves the reliability.

3. Design Considerations of the Proposed Converter

Based on the above analysis, the selection guidelines of the key parameters for the proposed converter are provided. The main specifications are as follows: output power P_o=3kW, input line-to-neutral voltage V_{in}=55V, output line-to-neutral voltage V_{out}=220V, line frequency f=50Hz, input power factor PF>0.92 and duty cycle D=0.5.

3.1 Input inductor selection

The input inductor is used to reduce the ripple of input current. In each module, the voltage across the inductor is equal to the input voltage during stage I. Therefore, the inductance L_{in} can be expressed as

$$L_{in} = \frac{DV_{in}}{\Delta i_{in} f_s} \tag{12}$$

where Δi_{in} is the input current ripple. Considering D=0.5, the minimum inductance can be represented by

$$L_{in} \geq \frac{3V_{in}^{\ 2}}{2P_o f_s \Delta i_{in}\%} \tag{13}$$

where Δi_{in}% is the ratio of Δi_{in} to the input current, which is taken the value of 0.2 in this paper.

3.2 Capacitance Calculation

Neglecting the conduction losses, the input reactive power of the proposed converter as shown in Figure 6 can be expressed as

$$Q_i = 6\pi f L_s I_{is}^{\ 2} - 6\pi f V_{os}^{\ 2} C_s \tag{14}$$

Furthermore, the input power factor PF is represented by

$$PF_i = \frac{P_i}{\sqrt{P_i^2 + Q_i^2}} \tag{15}$$

Based on the above equations and the requirement of the power factor, the maximum capacitance C_s can be obtained by

$$C_s = C_{eq} \le \frac{1}{6\pi f V_{os}{}^2}(6\pi f L_s I_{is}{}^2 + P_o \frac{\sqrt{1-PF_i^2}}{PF_i}) \tag{16}$$

Replacing equation (11) into (16), the maximum value for capacitors C_1 to C_{18} can be expressed as

$$C = \frac{8}{3}C_{eq} \le \frac{4}{9\pi f V_{os}{}^2}(6\pi f L_s I_{is}{}^2 + P_o \frac{\sqrt{1-PF_i^2}}{PF_i}) \tag{17}$$

In addition, the charging or discharging time interval must be less than 5τ to ensure that the SC cells can operate in PC mode, as mentioned earlier. Considering D=0.5 and substituting equation (8) into (6), the minimum capacitance can be represented by

$$C \ge \frac{0.1}{(2R_{DS(on)} + R_{ESR}) f_s} \tag{18}$$

3.3 Switches and Switching frequency

In order to obtain a low conduction resistance, a MOSFET IPDD60R037CM8, which has an $R_{DS(on)}$ value of 37mΩ, was selected to implement the unidirectional switches. By substituting the values of $R_{DS(on)}$, R_{ESR} and C into equation (18), the minimum switching frequency that ensures the converter operates in PC mode can be obtained by

$$f_{s\min} \ge \frac{0.1}{(2R_{DS(on)} + R_{ESR})C} \tag{19}$$

Furthermore, the feasibility of the switching frequency f_s in practical implementation should also be considered. Therefore, the switching frequency f_s was selected as 50kHz.

Parameters	Quantity	Values
Input line-to-neutral voltage (v_A, v_B, v_C)	-	55Vrms
Line frequency f	-	50Hz
Output power P_o	-	3000W
Output line-to-neutral voltage (v_R, v_S, v_T)	-	220Vrms
Switching frequency f_S	-	50kHz
Input inductor L_{in}	1	150µH
Capacitors (C_1~C_{18})	18	60µF/4mΩ
MOSFETs (S_1~S_{24})	24	37mΩ IPDD60R037CM8

Table 3. Main specifications and components of the prototype

4. Analysis Of Experimental Result

To demonstrate the previous analysis and operation of the proposed converter, a 3kW prototype is built as shown in Figure 7. The specific experimental parameters of the prototype, which are based on the methodology in section 3, are summarized in Table 3.

The experiments were conducted with D close to 0.5, and the input was fed by three-phase ac power. Figure 8 shows waveforms of the three line-to-neutral input voltages (v_A, v_B, and v_C) and one output voltage (v_R) for resistive load connected in a wye configuration. The output voltage v_R is in phase with the input voltage v_A. Furthermore, the amplitude of v_R is nearly four times that of v_A at D=0.5, which validates the voltage phase analysis in Figure 4. The line-to-neutral input voltages (v_A, v_B, and v_C) and line-to-line output voltage (v_{RS}) waveforms for the resistive load with delta connection are illustrated in Figure 9. As described in Figure 4, there is a 30° phase-shift between the v_{RS} and v_A, and the amplitude of v_{RS} is $4\sqrt{3}$ times that of v_A.

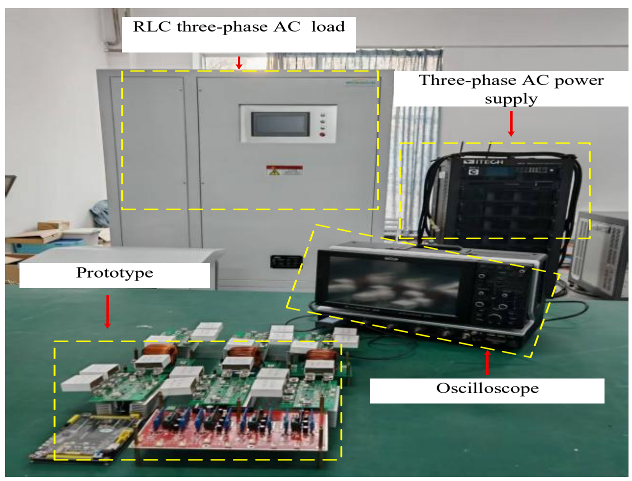

Figure 7. Picture of prototype.

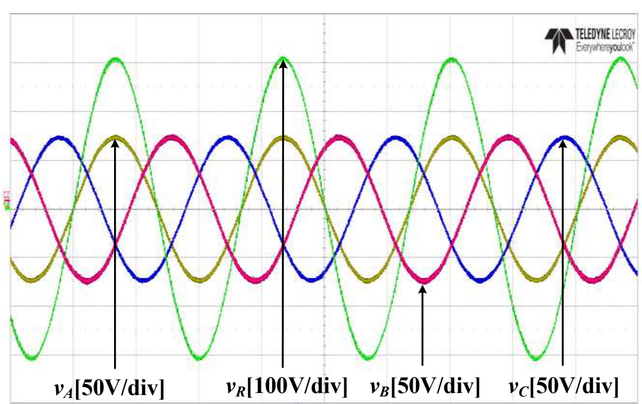

Figure 8. Experimental waveforms of output voltage v_R and input voltages v_A, v_B and v_C.

The line-to-neutral output voltages v_R, v_S, and v_T for the resistive load with a wye connection (48Ω per-phase) and line-to-neutral output current i_R are shown in Figure 10. It can be seen that i_R is in phase with v_R under the resistive load. Moreover, the output voltages v_R, v_S, and v_T are phase-shifted by 120° from each other.

Figure 11 illustrates the line-to-neutral output current i_R and line-to-neutral output voltages v_R, v_S, and v_T for the inductive load (0.61 power factor) with a wye connection. As expected, the current i_R under the inductive load lags behind output voltage v_R.

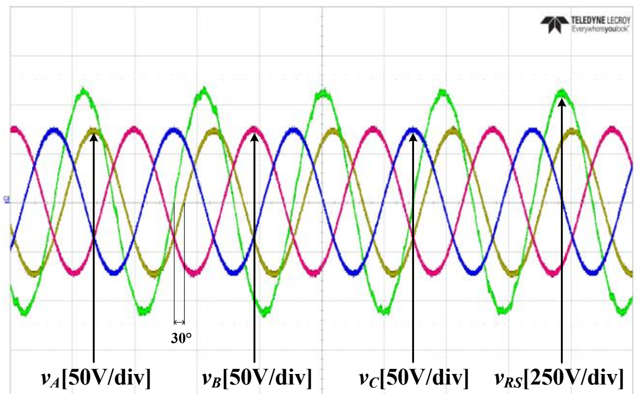

Figure 9. Experimental waveforms of output voltage v_{RS} and input voltages v_A, v_B and v_C.

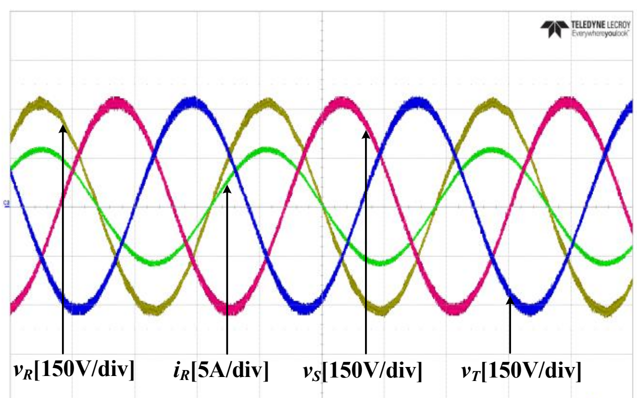

Figure 10. Experimental waveforms of line-to-neutral output voltages v_R, v_S, and v_T and line-to-neutral current i_R under resistive load.

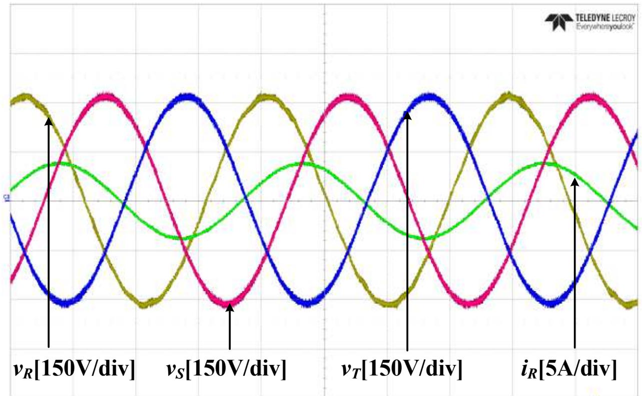

Figure 11. Experimental waveforms of line-to-neutral output voltages v_R, v_S, and v_T and line-to-neutral current i_R under inductive load.

The voltage waveforms for capacitors C_1, C_2 and C_3 in module A are shown in Figure 12. It can be observed that the capacitor voltages are approximately equal to half of the peak value of output voltage v_R, which is one of the advantages of this converter. Figure 13 shows capacitor voltages of C_1, C_7, and C_{13}. Since the capacitors are in different modules, their voltages have a phase shift of 120°. The voltages across S_1 and S_2 in module A are illustrated in Figure 14. Similarly, the voltage waveforms of switches exhibit the same characteristics as the corresponding capacitor voltages.

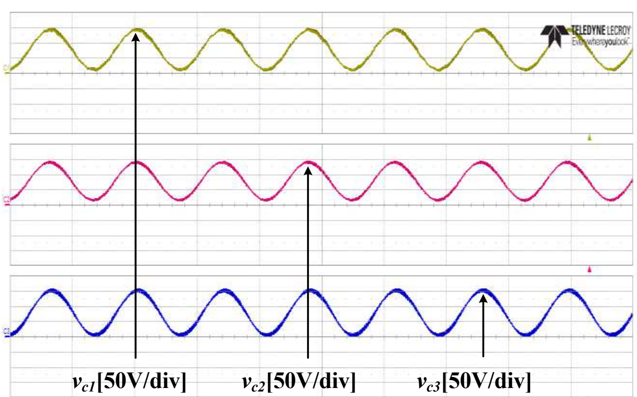

Figure 12. Experimental waveforms of capacitor voltages C_1, C_2, and C_3 in module A.

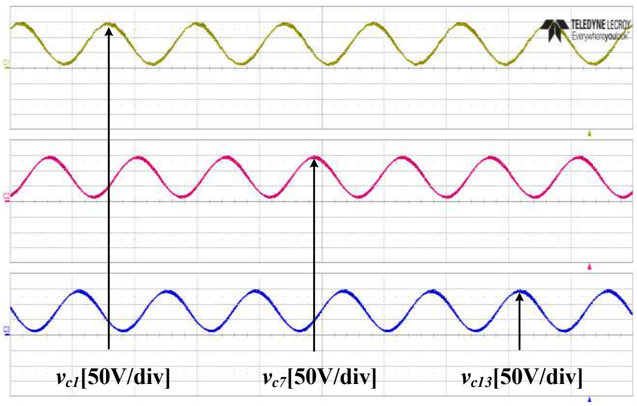

Figure 13. Experimental waveforms of capacitor voltages C_1, C_7, and C_{13}.

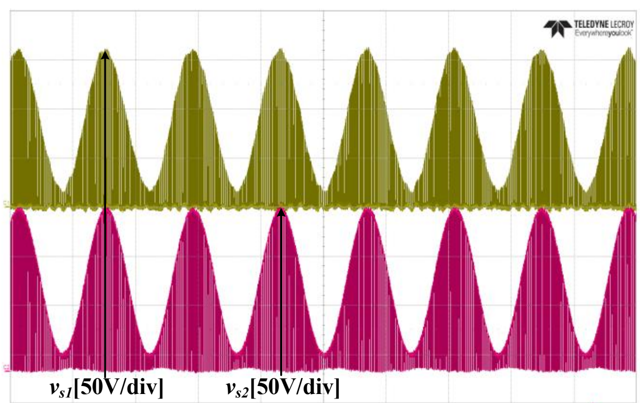

Figure 14. Experimental waveforms of switches S_1 and S_2 in module A.

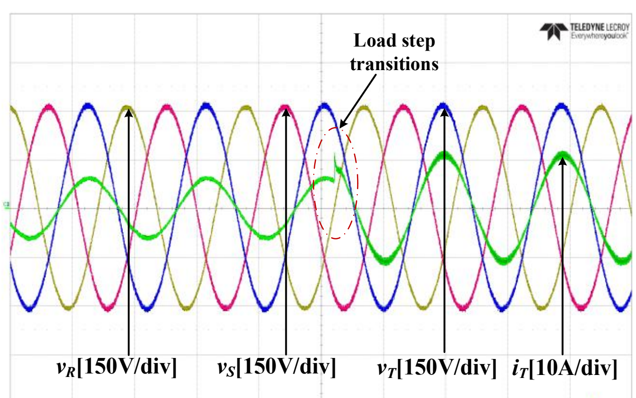

Figure 15. Experimental waveforms of line-to-neutral output voltages and line-to-neutral current for an unbalanced load.

The line-to-neutral output voltages and current for an unbalanced load are shown in Figure 15. Although one module handles more power than the other two (1kW for two modules and 2W for one module), the output voltages can still be maintained balanced. This is due to the self-balancing capability of capacitor voltages.

5. Conclusion

This paper proposes a three-phase ac/ac converter based on SC principle. The main features of this converter are simple modulation strategy, low voltage stresses across the components and capacitor voltage self-balancing capability. Because of the adoption of an input inductor, this converter can adjust the output voltage. Furthermore, the employment of unidirectional switches overcomes the commutation issues of bidirectional switches. The operation principle of the converter is analyzed. Subsequently, the quantitative analysis and design consideration are conducted. At last, the experimental results verify the theoretical analysis and its advantages. The proposed converter is suitable as an alternative to the conventional three-phase autotransformer.

Data availability

The data that support the findings of this study are available from the corresponding author on reasonable request.

References

1. Trindade, F. C. L., Nascimento, K. V. d. & Vieira, J. C. M. Investigation on Voltage Sags Caused by DG Anti-Islanding Protection. *IEEE Transactions on Power Delivery* **28**, 972-980, doi:10.1109/TPWRD.2012.2237419 (2013).
2. Strasser, T. *et al.* A Review of Architectures and Concepts for Intelligence in Future Electric Energy Systems. *IEEE Transactions on Industrial Electronics* **62**, 2424-2438, doi:10.1109/TIE.2014.2361486 (2015).
3. Newman, M. J., Holmes, D. G., Nielsen, J. G. & Blaabjerg, F. A dynamic voltage restorer (DVR) with selective harmonic compensation at medium voltage level. *IEEE Transactions on Industry Applications* **41**, 1744-1753, doi:10.1109/TIA.2005.858212 (2005).
4. Kaniewski, J., Szczesniak, P., Jarnut, M. & Benysek, G. Hybrid Voltage Sag\/Swell Compensators: A Review of Hybrid AC\/AC Converters. *IEEE Industrial Electronics Magazine* **9**, 37-48, doi:10.1109/MIE.2015.2404350 (2015).
5. Lo, K. Y. & Wang, W. Y. Bidirectional Isolated Single-Stage Single-Phase AC–AC Converter. *IEEE Journal of Emerging and Selected Topics in Power Electronics* **9**, 6828-6836, doi:10.1109/JESTPE.2021.3074307 (2021).
6. Nguyen, M. K., Jung, Y. G. & Lim, Y. C. Single-Phase AC–AC Converter Based on Quasi-Z-Source Topology. *IEEE Transactions on Power Electronics* **25**, 2200-2210, doi:10.1109/TPEL.2010.2042618 (2010).
7. Khan, A. A., Cha, H., Ahmed, H. F. & Kim, H. G. in *2016 IEEE 8th International Power Electronics and Motion Control Conference (IPEMC-ECCE Asia).* 1200-1205.
8. Costa, A. E. L. d., Jacobina, C. B., Rocha, N., Silva, E. R. C. d. & Filho, A. V. d. M. L. A Single-Phase ac–dc–ac Unidirectional Three-Leg Converter. *IEEE Transactions on Industrial Electronics* **68**, 3876-3886, doi:10.1109/TIE.2020.2987261 (2021).
9. Yang, L., Zhao, H., Wang, S. & Zhi, Y. Common-Mode EMI Noise Analysis and Reduction for AC–DC–AC Systems With Paralleled Power Modules. *IEEE Transactions on Power Electronics* **35**, 6989-7000, doi:10.1109/TPEL.2019.2957358 (2020).

10. Li, T. *et al.* Online Condition Monitoring of DC-Link Capacitor for AC/DC/AC PWM Converter. *IEEE Transactions on Power Electronics* **37**, 865-878, doi:10.1109/TPEL.2021.3092429 (2022).
11. Ebrahimian, A., Vahid, S., Weise, N. & Refaie, A. E.-. Two Level AC-DC-AC Converter Design with a New Approach to Implement Finite Control Set Model Predictive Control. *2021 22nd IEEE International Conference on Industrial Technology (ICIT).* 514-520.
12. Sun, Y. *et al.* Carrier-Based Modulation Strategies for Multimodular Matrix Converters. *IEEE Transactions on Industrial Electronics* **63**, 1350-1361, doi:10.1109/TIE.2015.2494871 (2016).
13. Qiu, L., Xu, L., Wang, K., Zheng, Z. & Li, Y. Research on Output Voltage Modulation of a Five-Level Matrix Converter. *IEEE Transactions on Power Electronics* **32**, 2568-2583, doi:10.1109/TPEL.2016.2581831 (2017).
14. Vijayagopal, M., Silva, C., Empringham, L. & Lillo, L. d. Direct Predictive Current-Error Vector Control for a Direct Matrix Converter. *IEEE Transactions on Power Electronics* **34**, 1925-1935, doi:10.1109/TPEL.2018.2833495 (2019).
15. Jayaprakasan, S., Ashok, S. & Ramchand, R. Analysis of Current Error Space Phasor for a Space Vector-Modulated Indirect Matrix Converter. *IEEE Transactions on Industrial Electronics* **69**, 4451-4459, doi:10.1109/TIE.2021.3078348 (2022).
16. Basu, K. & Mohan, N. A Single-Stage Power Electronic Transformer for a Three-Phase PWM AC/AC Drive With Source-Based Commutation of Leakage Energy and Common-Mode Voltage Suppression. *IEEE Transactions on Industrial Electronics* **61**, 5881-5893, doi:10.1109/TIE.2014.2311393 (2014).
17. Khan, A. A., Cha, H. & Kim, H. G. Magnetic Integration of Discrete-Coupled Inductors in Single-Phase Direct PWM AC–AC Converters. *IEEE Transactions on Power Electronics* **31**, 2129-2138, doi:10.1109/TPEL.2015.2427455 (2016).
18. Sharifi, S., Monfared, M. & Nikbahar, A. Highly Efficient Single-Phase Direct AC-to-AC Converter With Reduced Semiconductor Count. *IEEE Transactions on Industrial Electronics* **68**, 1130-1138, doi:10.1109/TIE.2020.2970652 (2021).
19. Jong-Hyun, K., Byung-Duk, M., Bong-Hwan, K. & Sang-Chul, W. A PWM buck-boost AC chopper solving the commutation problem. *IEEE Transactions on Industrial Electronics* **45**, 832-835, doi:10.1109/41.720341 (1998).
20. Kolar, J. W., Schafmeister, F., Round, S. D. & Ertl, H. Novel Three-Phase AC–AC Sparse Matrix Converters. *IEEE Transactions on Power Electronics* **22**, 1649-1661, doi:10.1109/TPEL.2007.904178 (2007).
21. Rodriguez, J., Rivera, M., Kolar, J. W. & Wheeler, P. W. A Review of Control and Modulation Methods for Matrix Converters. *IEEE Transactions on Industrial Electronics* **59**, 58-70, doi:10.1109/TIE.2011.2165310 (2012).
22. Empringham, L., Kolar, J. W., Rodriguez, J., Wheeler, P. W. & Clare, J. C. Technological Issues and Industrial Application of Matrix Converters: A Review. *IEEE Transactions on Industrial Electronics* **60**, 4260-4271, doi:10.1109/TIE.2012.2216231 (2013).
23. Hoyo, J., Alcala, J. & Calleja, H. A high quality output AC/AC Cuk converter. *2004 IEEE 35th Annual Power Electronics Specialists Conference (IEEE Cat. No.04CH37551).* 2888-2893 Vol.2884.
24. Tang, Y., Zhang, C. & Xie, S. Z-Source AC-AC Converters Solving Commutation Problem. *2007 IEEE Power Electronics Specialists Conference.* 2672-2677.
25. He, L., Duan, S. & Peng, F. Safe-Commutation Strategy for the Novel Family of Quasi-Z-Source AC–AC Converter. *IEEE Transactions on Industrial Informatics* **9**, 1538-1547, doi:10.1109/TII.2013.2245333 (2013).
26. Ahmed, H. F., Cha, H., Khan, A. A. & Kim, H. G. A Family of High-Frequency Isolated Single-Phase Z-Source AC–AC Converters With Safe-Commutation Strategy. *IEEE Transactions on Power Electronics* **31**, 7522-7533, doi:10.1109/TPEL.2016.2539216 (2016).
27. Umeno, T., Takahashi, K., Oota, I., Ueno, F. & Inoue, T. New Switched-Capacitor DC-DC Converter with Low Input Current Ripple and Its Hybridization. *Proceedings of the 33rd Midwest Symposium on Circuits and Systems.* 1091-1094 vol.1092.
28. Ioinovici, A. Switched-capacitor power electronics circuits. *IEEE Circuits and Systems Magazine* **1**, 37-42, doi:10.1109/7384.963467 (2001).
29. Ben-Yaakov, S. & Evzelman, M. Generic and unified model of Switched Capacitor Converters. *2009*

IEEE Energy Conversion Congress and Exposition. 3501-3508.

30. Ben-Yaakov, S. Behavioral Average Modeling and Equivalent Circuit Simulation of Switched Capacitors Converters. *IEEE Transactions on Power Electronics* **27**, 632-636, doi:10.1109/TPEL.2011.2171996 (2012).
31. Evzelman, M. & Ben-Yaakov, S. Average-Current-Based Conduction Losses Model of Switched Capacitor Converters. *IEEE Transactions on Power Electronics* **28**, 3341-3352, doi:10.1109/TPEL.2012.2226060 (2013).
32. Kimball, J. W. & Krein, P. T. Analysis and design of switched capacitor converters. *Twentieth Annual IEEE Applied Power Electronics Conference and Exposition, 2005. APEC 2005.* 1473-1477 Vol. 1473.
33. Kimball, J. W., Krein, P. T. & Cahill, K. R. Modeling of capacitor impedance in switching converters. *IEEE Power Electronics Letters* **3**, 136-140, doi:10.1109/LPEL.2005.863603 (2005).
34. Cheung, C. K., Tan, S. C., Tse, C. K. & Ioinovici, A. On Energy Efficiency of Switched-Capacitor Converters. *IEEE Transactions on Power Electronics* **28**, 862-876, doi:10.1109/TPEL.2012.2204903 (2013).
35. Lazzarin, T. B., Andersen, R. L., Martins, G. B. & Barbi, I. A 600-W Switched-Capacitor AC–AC Converter for 220 V/110 V and 110 V/220 V Applications. *IEEE Transactions on Power Electronics* **27**, 4821-4826, doi:10.1109/TPEL.2012.2203318 (2012).
36. Andersen, R. L., Lazzarin, T. B. & Barbi, I. A 1-kW Step-Up/Step-Down Switched-Capacitor AC–AC Converter. *IEEE Transactions on Power Electronics* **28**, 3329-3340, doi:10.1109/TPEL.2012.2222674 (2013).
37. Dall'Asta, M. S., Barbi, I. & Lazzarin, T. B. AC–AC Hybrid Boost Switched-Capacitor Converter. *IEEE Transactions on Power Electronics* **35**, 13115-13125, doi:10.1109/TPEL.2020.2992490 (2020).
38. Lazzarin, T. B., Andersen, R. L. & Barbi, I. A Switched-Capacitor Three-Phase AC–AC Converter. *IEEE Transactions on Industrial Electronics* **62**, 735-745, doi:10.1109/TIE.2014.2336625 (2015).
39. Vecchia, M. D., Lazzarin, T. B. & Barbi, I. A Three-Phase AC–AC Converter in Open-Delta Connection Based on Switched Capacitor Principle. *IEEE Transactions on Industrial Electronics* **62**, 6035-6041, doi:10.1109/TIE.2015.2426673 (2015).
40. Silva, R. L. d., Lazzarin, T. B. & Barbi, I. Reduced Switch Count Step-Up/Step-Down Switched-Capacitor Three-Phase AC–AC Converter. *IEEE Transactions on Industrial Electronics* **65**, 8422-8432, doi:10.1109/TIE.2018.2808900 (2018).
41. Shin, H. H., Cha, H., Kim, H. G. & Yoo, D. W. Novel Single-Phase PWM AC–AC Converters Solving Commutation Problem Using Switching Cell Structure and Coupled Inductor. *IEEE Transactions on Power Electronics* **30**, 2137-2147, doi:10.1109/TPEL.2014.2330351 (2015).
42. Mayo-Maldonado, J. C. *et al.* A contribution to the dynamic modeling of switched-capacitor converters. *2011 IEEE Energy Conversion Congress and Exposition.* 1284-1290.

Acknowledgements

All authors of this paper would like to thank all the participants who have improved the quality of this work.

Author contributions

G.Y.Y. designed the topology and drafted the manuscript. R.Y.L. designed and completed the experiment. C.L. provided necessary resources for the research. D.B.G. analyzed the operational principle. M.L.H. participated in deriving formulas related to operational analysis. F.Y.Z. participated in the simulation modeling of the topology. All authors reviewed the manuscript.

Funding

This work is supported by Scientific Research Project of Jilin Province Department of Education (JJKH20250865KJ) and The National Natural Science Foundation of China (52407195).

Competing interests

The authors declare no competing interests.

Figure legends

Figure 1. (a) Proposed SC three-phase ac/ac converter; (b) PWM drive signals; (c) Simplified symbol for a module.

Figure 2. Operational stages for module A. (a) Stage I: even switches are in on-state; (b) Stage II: odd switches are in on-state. Circulating path for the inductor current i_L during dead time. (c) $i_L>0$; (d) $i_L<0$.

Figure 3. Theoretical voltage waveforms of the proposed converter. (a) Input voltages; (b) Output voltages; (c) Voltages across capacitors; (d) Voltages across switches.

Figure 4. Analysis of voltage phasor for different module-load connections(D=0.5).

Figure 5. Three-phase equivalent circuit for wye-wye connection.

Figure 6. Proposed single-phase equivalent circuit.

Figure 7. Picture of prototype.

Figure 8. Experimental waveforms of output voltage v_R and input voltages v_A, v_B and v_C.

Figure 9. Experimental waveforms of output voltage v_{RS} and input voltages v_A, v_B and v_C.

Figure 10. Experimental waveforms of line-to-neutral output voltages v_R, v_S, and v_T and line-to-neutral current i_R under resistive load.

Figure 11. Experimental waveforms of line-to-neutral output voltages v_R, v_S, and v_T and line-to-neutral current i_R under inductive load.

Figure 12. Experimental waveforms of capacitor voltages C_1, C_2, and C_3 in module A.

Figure 13. Experimental waveforms of capacitor voltages C_1, C_7, and C_{13}.

Figure 14. Experimental waveforms of switches S_1 and S_2 in module A.

Figure 15. Experimental waveforms of line-to-neutral output voltages and line-to-neutral current for an unbalanced load.